Development of a Coupled Hydro-Economic Model to Support Groundwater Irrigation Decisions

Boyao Tian [1] *

Andrea Brookfield [1]

Margaret Insley [2]

[1]Department of Earth and Environmental Sciences, University of Waterloo, 200 University Avenue West, Waterloo, ON, Canada, N2L 3G1.

[2]Department of Economics, University of Waterloo, 200 University Avenue West, Waterloo, ON, Canada, N2L 3G1.

[1]* Corresponding Author: boyao.tian@uwaterloo.ca

Abstract

Groundwater sustains global agriculture but faces significant pressure from overexploitation, threatening long-term water security. Achieving a balance between agricultural productivity and sustainable groundwater use requires decision-support tools that are both practical and robust. This study develops an accessible farm-level hydro-economic model that integrates groundwater dynamics with economic outcomes to evaluate irrigation strategies under regulatory and physical constraints. The model estimates land value over time while incorporating uncertain precipitation, irrigation practices, and regulatory limits. This research presents a novel application of Conditional Value-at-Risk to assess economic risk of groundwater irrigation by focusing on the tail of the probability curve, emphasizing potential extreme adverse outcomes rather than average performance. Applied to a representative High Plains Aquifer site, the model shows that more pumping does not guarantee greater profitability, as diminishing returns and aquifer depletion can undermine long-term benefits. Instead, irrigation strategies aligned with site-specific aquifer properties and regulatory thresholds improve both economic performance and sustainability. This scalable approach provides a practical framework to inform irrigation policy, support farmer decision-making, and promote sustainable groundwater under growing uncertainty.

Keywords: Groundwater Management; Integrated Hydrologic Models; Conditional Value-at-Risk; Dynamic Model; Analytical Models

Highlights:

- Farm-level model quantifies economic and hydrologic impacts of irrigation.
- Irrigation strategies affect both short-term returns and long-term sustainability.
- Increased irrigation beyond a site-specific limit shows diminishing economic gains.
- CVaR highlights downside irrigation risks.
- Model supports farmer and regulator decisions under water constraints.

1 Introduction

Groundwater supports ecosystems and human health and plays an important role in agricultural water supply. The increasing global food demand driven by population and income growth poses a significant challenge to agricultural water usage (Mancosu et al., 2015; Fróna et al., 2019; Hemathilake and Gunathilake, 2022). The use of groundwater for irrigation is increasing both in absolute terms and as a percentage of total irrigation, leading to groundwater depletion in regions where groundwater extraction is greater than groundwater recharge (Siebert et al., 2010; Jia et al., 2020). In many areas of the world, groundwater depletion has reached critical levels, forcing reductions in irrigation and subsequently crop growth (Sacks et al., 2009; Aeschbach-Hertig and Gleeson, 2012). The effects of groundwater depletion can lead to significant economic losses for the agricultural industry, reduced environmental sustainability, and increased competition between water users (Jain et al., 2021; Mukherjee et al., 2021). These consequences can result in severe conflicts over water resources (Tzanakakis et al., 2020; Akhtar et al., 2021).

The integration of hydrologic models and economic methods has been applied widely in agriculture, water management, and policy design, e.g., Ding and Peterson (2012); Edwards (2016); Guilfoos et al. (2016); Oehninger and Lawell (2019); Amaya et al. (2021); and Genova and Wei (2023); and the effect of risk and uncertainty on optimal groundwater use and regulation has also been a focus in the literature: Katic and Grafton (2011); Merrill and Guilfoos (2018); and Escriva-Bou et al. (2020). However, none of these approaches fully account for tail risk by incorporating the less probable, yet potentially most economically severe, events.

This paper contributes to the literature by developing a novel coupled hydro-economic model that assesses the economic implications and tail risk of groundwater pumping decisions at the farm level. Under stochastic precipitation and regulatory constraints, the model

estimates groundwater availability and expected land values while employing Conditional Value-at-Risk (CVaR) to assess potential risks.

CVaR is a widely used risk assessment tool in finance that accounts for the entire distribution of potential losses, emphasizing tail risk (Rockafellar and Uryasev, 2000, 2002). Compared to traditional risk measures like simple standard deviation or Value-at-Risk (VaR), CVaR provides a more robust evaluation of uncertainties, making it a preferred approach in decision-making under risk (Rockafellar and Uryasev, 2000, 2002; Sarykalin et al., 2008; Filippi et al., 2020). Beyond finance, CVaR has been applied in diverse fields, including inventory management (Gotoh and Takano, 2007; Zhang et al., 2009), supply chain management (Wu and Blackhurst, 2009; Sawik, 2019), transportation (Toumazis and Kwon, 2013; Ansaripoor et al., 2014), energy (Pousinho et al., 2011; Hosseini-Firouz, 2013), and medicine (Romeijn et al., 2006; Filippi et al., 2020). However, its application in agriculture, particularly in groundwater management, remains largely unexplored. Given the increasing uncertainty in water availability due to climate change and competing demands, integrating CVaR into agricultural water management presents a valuable opportunity to enhance risk-informed decision-making. Furthermore, CVaR's effectiveness in optimization problems makes it a promising tool for future extensions of this model, enabling more adaptive and resilient strategies for sustainable groundwater use in agriculture.

The primary objectives of this study are (1) to build a practical and accessible hydro-economic model focusing on groundwater availability and expected land values at a farm level; (2) to introduce CVaR analysis to quantify economic risk associated with variability in precipitation and crop price; and (3) to evaluate how different irrigation decisions affect farm value, using Monte Carlo simulations to identify optimal strategies. To our knowledge, this represents the first application of CVaR in agricultural groundwater use, providing a new approach for assessing risk in groundwater-dependent farming. The outcomes can provide valuable insights into the sustainable use of groundwater resources in agriculture and

contribute to the formulation of effective strategies for future agricultural water management.

2 Methods

This section presents the equations for the precipitation model, groundwater model, crop yield model, economic model, and risk assessment model, with the overall workflow illustrated in Figure 1. To simplify, we use two conceptual hydrologic models (Figure 2) representing common aquifer conceptualizations, confined and unconfined single-layer aquifers. All model components are applicable to both conditions, with differences in parameters such as specific yield or storativity explicitly stated in corresponding sections.

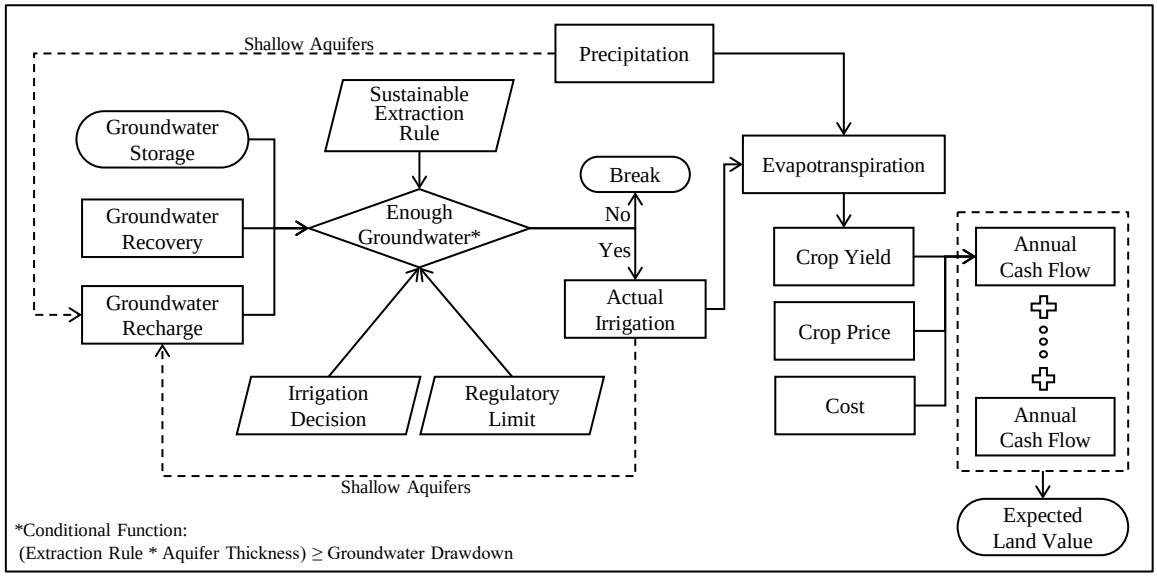

Figure 1: Workflow of the hydro-economic model developed in this work. "Aquifer thickness" in conditional function refers to the aquifer thickness for unconfined aquifers and hydraulic head for confined aquifers.

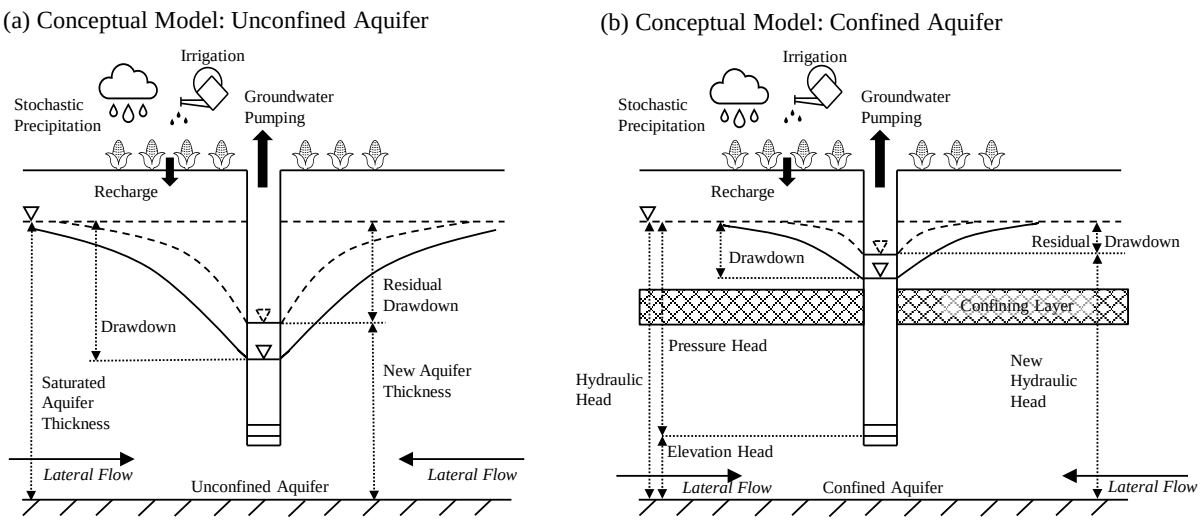

Figure 2: Conceptual hydrologic models illustrating the processes included in this study: (a) unconfined aquifer; (b) confined aquifer.

2.1 Precipitation Model

Monthly precipitation is simulated using a simple first-order Markov chain exponential model based on Richardson (1981). This method describes the occurrence of wet or dry months and then uses an exponential distribution function to predict the amount of precipitation. In this model, a month with a total rainfall of 6 mm or more is considered a wet month (Richardson, 1981). $P_i(W/D)$ is the probability of a wet month in month i given a dry month in month i-1.; $P_i(W/W)$ is the probability of a wet month in month i given a wet month in month i-1. Conversely, $P_i(D/D)$ is the probability of a dry month in month i given a dry month in month i-1; $P_i(D/W)$ is the probability of a dry month in month i given a wet month in month i-1. The relationships between these probabilities are:

$$P_i(W/D) + P_i(D/D) = 1 \tag{1}$$

$$P_i(W/W) + P_i(D/W) = 1 \tag{2}$$

Rainfall depth is analyzed using an exponential distribution, with the probability density function ($f(R)$) given by:

$$f(R) = \lambda\, e^{-\lambda R} \tag{3}$$

where λ is the distribution parameter $[L^0]$, which is calculated by dividing the total precipitation amount for either wet or dry months by the number of corresponding months; R is the precipitation amount $[L]$. A series of statistical tests and Monte Carlo simulations were conducted to assess the precipitation model's performance, which is provided in Appendix A.1, Figure A-1.

2.2 Groundwater Model

The groundwater model developed for this study simulates recharge, recovery, and resulting groundwater storage, and estimates drawdown due to pumping to assess whether aquifer thickness (or hydraulic head) is sufficient for the next growing season. Designed as a practical and accessible tool, this analytical model provides a simplified alternative to complex numerical models, requiring less data and offering greater accessibility for policymakers and stakeholders. Since it is difficult to determine the specific area from where water is pumped within an aquifer, this model simplifies the water volume by considering changes in aquifer thickness (or hydraulic head) only, assuming an infinite areal extent. All the equations are on a yearly basis. We focus only on groundwater, excluding groundwater-surface water interactions at this time.

2.2.1 Groundwater Recharge

Groundwater recharge occurs as water moves from land surface through pore spaces down to the water table, which is primarily composed of infiltration of precipitation and local surface waters (Meixner et al., 2016). In addition, some water applied for irrigation

also percolates downward below the root zone and recharges the aquifer (Miller and Appel, 1997). Here, we use two methods to estimate recharge (R_{ch}):

$$R_{ch} = \begin{cases} R_I + R_P, & \text{shallow aquifer only} \\ R_{ch}(t) \end{cases} \tag{4}$$

For shallow aquifers or those with fast recharge times, recharge is divided into two sources: from irrigation (R_I $[LT^{-1}]$ and from precipitation (R_P $[LT^{-1}]$). This model assumes that R_I is the portion of irrigation water not used by evapotranspiration or surface runoff and is represented by: $R_I = I_d * (1 - I_e - I_{rf})$, where I_d is the irrigation water applied $[LT^{-1}]$, I_e is the irrigation efficiency $[L^0]$, I_{rf} is the percentage of irrigation runoff $[L^0]$. Similarly, recharge from precipitation is calculated as the precipitation remaining after ET and surface runoff: $R_P = P_Y * (1 - P_e - P_{rf})$, where P_Y is the yearly precipitation $[LT^{-1}]$, P_e is the precipitation efficiency $[L^0]$, P_{rf} is the percentage of precipitation runoff $[L^0]$. Appropriate values of these parameters can be chosen based on the characteristics of specific sites.

Another option for recharge is to use a temporally variable rate provided by the user, which is particularly useful for deeper aquifers and those with long and complex recharge pathways. In deeper aquifers, there is often a significant delay in water recharging to the aquifer. For instance, in the High Plains Aquifer (HPA), it can take hundreds of years for recharge to reach the aquifer (Schwartz and Ibaraki, 2011; Cotterman et al., 2018). In these cases, a more accessible option is to set a prescribed recharge value (either constant or variable in time), as the aquifer depth minimizes the direct influence of weather or irrigation on recharge rates, and the influence of diffuse and focused recharge pathways are complex to discern. Regional estimates are often available in the literature, such as those for the HPA from Sophocleous (2005); Gurdak and Roe (2010); Sophocleous (2010); Crosbie et al. (2013) and other cases from Cao et al. (2013); Konikow (2015).

2.2.2 Groundwater Drawdown

Groundwater drawdown refers to the lowering of the water table due to groundwater withdrawal. Analytical solutions developed by Cooper and Jacob (1946) and their corrections are used to calculate the drawdown due to pumping in a single well (Driscoll, 1986; Brookfield, 2016):

$$S_{aquifer} = \frac{Q}{4\pi T_{aquifer}} \left[-0.5772 - \ln\left(\frac{r_w^2 S}{4 T_{aquifer} t_p} \right) \right] \tag{5}$$

where $S_{aquifer}$ is the drawdown in the aquifer over a pumping duration $[L]$, Q is the pumping rate $[L^3T^{-1}]$, r_w is the effective radius of the well $[L]$, S is the storativity $[L^0]$, t_p is the duration of pumping $[T]$. $T_{aquifer}$ is transmissivity $[L^2T^{-1}]$, given by $T_{aquifer} = Kb$, where K is the hydraulic conductivity $[LT^{-1}]$, and b is the aquifer thickness $[L]$.

Equation (5) represents drawdown under the assumption that hydraulic head does not change with pumping (i.e., in a confined aquifer). For unconfined aquifers, we use specific yield (s_y $[L^0]$) instead of storativity and account for thickness variations; other adjustments for well efficiency and neighboring well impacts are provided in Appendix A.2. Validation of the analytical method's implementation is provided in Appendix A.2, Figure A-2.

2.2.3 Groundwater Recovery

This model assumes that groundwater pumping occurs only during the growing season. However, recovery begins simultaneously with pumping and is also influenced by when pumping ceases during the non-growing season. Theis (1935) proposed the concept of recovery, or residual drawdown (s' $[L]$):

$$s' = \frac{2.30 Q_d}{4\pi T_{aquifer}} log_{10} \frac{t_s}{t_c} \tag{6}$$

where Q_d is the discharge rate $[L^3T^{-1}]$; t_s is the time in days since the start of pumping $[T]$; t_c is the time in days since the cessation of pumping $[T]$. This model assumes zero

natural discharge from the aquifer; therefore, it is assumed that this discharge rate equals the pumping rate ($Q_d = Q$). Although this method is used for confined aquifers, it is applicable in unconfined aquifers for late-time recovery data (Neuman, 1975). Validation of the analytical method's implementation is provided in Appendix A.3, Figure A-3.

2.3 Crop Yield Model

The crop yield model is based on two main components: evapotranspiration estimated using the FAO Penman-Monteith approach (Allen et al., 1998) and crop yield estimation from Martin et al. (2010) and Klocke (2011).

2.3.1 Evapotranspiration

Evaporation and transpiration occur simultaneously, and they are commonly referred to as evapotranspiration (ET), which directly effects crop yield and is influenced by climate, crop characteristics, and environmental factors (Allen et al., 1998). In this model, ET reflects crop growth status after receiving water from precipitation and irrigation and is used for further prediction of yield. To calculate potential evapotranspiration for a specific crop, reference evapotranspiration (ET_r $[LT^{-1}]$) must first be estimated, using the FAO Penman-Monteith Equation (Allen et al., 1998):

$$ET_r = \frac{0.408\Delta(R_n - G) + \gamma\frac{900}{T_{air}+273}u_2(e_s - e_a)}{\Delta + \gamma(1 + 0.34u_2)} \tag{7}$$

where Δ is the slope of the vapor pressure curve $[ML^{-1}T^{-2}\theta^{-1}]$; R_n is the net radiation at the crop surface $[MT^{-3}]$; G is the soil heat flux $[MT^{-3}]$; γ is the psychrometric constant $[ML^{-1}T^{-2}\theta^{-1}]$; T_{air} is the average air temperature $[\Theta]$; u_2 is the wind speed at 2 m height $[LT^{-1}]$; e_s is saturation vapour pressure $[ML^{-1}T^{-2}]$; e_a is actual vapour pressure $[ML^{-1}T^{-2}]$.

Potential ET (ET_p $[LT^{-1}]$) is then calculated from ET_r using a daily crop coefficient (K_c $[L^0]$). Suitable values of K_c for a variety of crops and land cover are available in published literature (e.g., Allen et al. (1998)).

$$ET_p = K_c ET_r \tag{8}$$

2.3.2 Crop yield

In this research, a commonly used yield function, modified by Martin et al. (2010) and Klocke (2011), is chosen to estimate crop yield. This mathematical model aligns well with observed data and effectively captures the diminishing returns of yield gains as additional inputs are applied (Klocke, 2011).

$$Y_a = Y_n + b_{slope} ET_{inc} \left[1 - \left(1 - \frac{I_d}{I_r} \right)^{\frac{1}{I_e}} \right] \tag{9}$$

where Y_a is the estimated yield $[ML^{-2}T^{-1}]$; Y_n is the non-irrigated yield that is produced from precipitation only $[ML^{-2}T^{-1}]$; b_{slope} is the slope of the yield-evapotranspiration function $[ML^{-3}]$; ET_{inc} is the difference between the amount of water used by a fully irrigated crop for maximum yield (ET_p) and the amount of water used by a non-irrigated crop, assuming equals effective precipitation during the growing season (P_E) $[LT^{-1}]$; I_r is the amount of irrigation required to produce maximum yield $[LT^{-1}]$. Validation of this method is provided in Appendix A.4, Figure A-4; and the estimated annual yield is shown in Figure A-5, aligning with the exponential component of the yield function.

2.3.3 Maximum Crop Irrigation Requirement

The maximum crop irrigation requirement indicates the amount of irrigation needed to match the ET_p per year. Therefore, I_r for each year can be written as:

$$I_r = \frac{ET_p - P_E}{I_e} \tag{10}$$

2.3.4 Available Water

As mentioned at the beginning of this section, to simplify calculations and avoid the need to specify the pumping area, this model uses total available aquifer thickness (or hydraulic head), denoted as b $[L]$, at the beginning of each growing season to represent available groundwater storage. Assuming yearly time steps Δt, aquifer thickness is updated as:

$$b_t = b_{t-1} - s'\Delta t + R_{ch}\Delta t \tag{11}$$

Additionally, this model incorporates a sustainable extraction rule (μ), representing the maximum allowable decline in aquifer thickness (or hydraulic head), expressed as a percentage of the initial thickness. This is one possible regulatory approach to promote long-term groundwater sustainability. Detailed explanations of μ are also provided in Section 3.3.

Following Butler Jr et al. (2020) work, the model also enforces a minimum aquifer thickness of 8 meters, below which pumping becomes technically infeasible. Therefore, groundwater extraction can proceed only if all three constraints are satisfied: (1) drawdown does not exceed the allowable sustainable extraction limit, (2) the updated aquifer thickness remains above the residual portion of the sustainable extraction limit, and (3) the minimum threshold of 8 m is maintained. These constraints ensure that pumping is not a fixed or arbitrary value, but a dynamic outcome determined by both hydrologic feedbacks and regulatory boundaries. This structure allows the model to capture realistic fluctuations in water

availability and emphasize the adaptive nature of irrigation decisions under physical and policy-driven limitations.

2.4 Economic Model

In this model, the state variables are precipitation $P_E(t)$, crop price $P(t)$, available water in the aquifer $B(t)$, and irrigation requirement for maximum yield $I_r(t)$. The control variable is the farmer's decision on the irrigation fraction β, which represents the proportion of crop water demand met by irrigation. This economic model estimates the expected land value of a farm over a planning horizon T, including a crop price model, cost function, and irrigation strategies. Actual irrigation water applied is determined by crop water demand, groundwater availability, and operational constraints.

2.4.1 Price Model

This work uses a Mean Reverting (MR) process to simulate crop prices, which is a stochastic process commonly used to model commodity prices (Insley, 2002; Zhang et al., 2015). The MR price is given by:

$$dP_t = \theta(\bar{P} - P_t)dt + \sigma_m P_t dz_t \tag{12}$$

where P_t is the crop price [unit of local currency] at time t; θ is the speed of mean reversion $[L^0]$; $\bar{P}$ is the long-run mean or equilibrium of the crop price [unit of local currency]; σ_m is the volatility $[L^0]$; dz_t is an increment in a stochastic process z that follows the standard Brownian motion. The discrete time approximation of this approach is provided by:

$$P_t - P_{t-1} = \theta\bar{P}\Delta t - \theta\Delta t P_{t-1} + \sigma_m P_{t-1}\sqrt{\Delta t}\epsilon_t \tag{13}$$

where Δt is time step size, 1/12 year. Ordinary least squares regression (Insley and Wirjanto, 2010) is used to estimate the coefficients, c(1) and c(2):

$$\frac{P_t - P_{t-1}}{P_{t-1}} = c(1) + c(2)\frac{1}{P_{t-1}} \tag{14}$$

Where $\theta = \frac{-c(1)}{\Delta t}$, $\sigma_m = \frac{se_m}{\sqrt{\Delta t}}$, $\bar{P} = \frac{c(2)}{\theta \Delta t}$. Estimates of these values are provided in Appendix B. Price validation and estimations of 10,000 Monte Carlo simulation are provided in Appendix C.

2.4.2 Cost Functions

The cost includes three components: fixed costs (C_f), which remain constant regardless of yield or pumping, such as land and machinery costs; harvest costs (C_y), simplified here as fertilizer expenses, which are directly related to crop yield; and pumping costs, which depend on both energy prices (C_e) and energy usage. Pumping cost modified from Alam et al. (2023) is given as:

$$Energy\,Cost * Energy\,Usage = C_e \frac{V_a \Delta H \rho g}{3.6 \times 10^6 \eta_p} \tag{15}$$

where, C_e is the cost of electricity [unit of local currency]; V_a is the pumping volume $[L^3]$; ΔH is the distance for lifting water from aquifers to the ground surface $[L]$, which is determined by each year's groundwater level; ρ is the water density $[ML^{-3}]$; g is the gravity factor $[LT^{-2}]$; η_p is the pumping efficiency $[L^0]$.

2.4.3 Irrigation Decision

In this model, the farmer's irrigation decision is based on a proportional rule:

$$I_d(t) = \beta * I_r(t), \qquad \beta \in (0, 1] \tag{16}$$

where β is the control variable, while $I_d(t)$ is the resulting irrigation volume determined by the chosen β and the given crop water required to reach maximum yield $I_r(t)$ each year (Equation 10). Although β could exceed 1 technically (pumping more than the crop water demand), such over-irrigation is generally undesirable due to potential yield losses, unnecessary pumping costs, and inefficient water use. Therefore, we restrict $\beta \in (0, 1]$, e.g., $\beta = 1$ corresponding to full irrigation and $\beta = 0.9$ representing 90% of demand. The actual irrigation applied in period t, $I_a(t)$, is the minimum of the farmer's decision $I_d(t)$ as determined by the control variable β; the available groundwater storage $B(t)$; and the regulatory pumping limit $\bar{I}(t)$:

$$I_a(t) = min(I_d(t), \bar{I}(t), B(t)) \tag{17}$$

This research evaluates alternative profiles for the regulatory limit $\bar{I}(t)$ to represent different policy scenarios. These include (i) a constant regulatory pumping limit (Q_c) over the entire planning horizon (T), and (ii) a time-varying regulatory pumping limit (Q_n), where the pumping limit can shift at specified breakpoints (τ) (e.g., by third, or half of the horizon). This allows exploration of different regulatory rules that might be imposed including both decreasing and increasing water use over time, as well as more complex stepwise rules:

$$\text{(i) Constant regulatory pumping limit:} \quad \bar{I}(t) = Q_c, \quad \forall t \in T \tag{18}$$

$$\text{(ii) Time-varying regulatory pumping limit:} \quad \bar{I}(t) = \begin{cases} Q_1, & t \in (0, \tau_1] \\ Q_2, & t \in (\tau_1, \tau_2] \\ \vdots & \\ Q_n, & t \in (\tau_{n-1}, T] \end{cases} \tag{19}$$

These formulations emphasize that actual irrigation depends jointly on the farmer's decision,

physical constraints, and policy constraints, resulting in a dynamic year-to-year adjustment of pumping.

2.4.4 Expected Land Values

The land value function V depends on key state variables and the farmer's control at each time t. Specifically, V is expressed as a function of precipitation $P_E(t)$, crop price $P(t)$, available groundwater in the aquifer $B(t)$, irrigation required for maximum yield $I_r(t)$, farmer's irrigation decision β, and time t, and denoted as $V(P_E, P, B, I_r, t; \beta)$. These relationships show the dynamic linkage between environmental conditions, farmer decisions, and economic outcomes.

Annual cash flow ($\pi(t)$) is determined by crop yield, crop price, and associated costs. Crop yield $Y_a(t)$, determined by stochastic precipitation $P_E(t)$ and irrigation water applied $I_a(t)$, corresponds to the actual crop yield estimated by Equation (9):

$$Y_a(t) = Y_a(P_E(t), I_a(t), t)dt \tag{20}$$

As a result, the annual cash flow is:

$$\pi(t) = Y_a(t) * (P(t) - C_y) - C_f * Area - C_e * Energy\,Usage \tag{21}$$

Then, the present value in year $t = t_i$ of annual cash flow in some future year $t = t'$ is calculated using a discount rate, r $[L^0]$, by:

$$e^{-r(t'-t_i)}\pi(t') \tag{22}$$

Therefore, the expected value of the farm in year t_i is the expected present value of

all cash flows from time t to the end date, denoted T; where p_e, p, b, ι denote particular realizations of the state variables P_E, P, B, I_r at time t_i.

$$V(p_e, p, b, \iota, t_i; \beta) = \sup \mathbb{E}\left[\int_{t=t_i}^{T} e^{-rt}\pi\big(P_E(t), P(t), B(t), I_r(t), t; \beta\big)dt \,\middle|\, P_E(t_i) = p_e, P(t_i) = p, B(t_i) = b, I_r(t_i) = \iota, t = t_i\right] \tag{23}$$

2.5 Risk Assessment Model

Risk in agricultural decisions can be characterized in multiple ways. Standard deviation captures overall variability, highlighting strategies that yield high returns in good years but large variations in outcomes. However, it does not distinguish between upside and downside variability, making it a limited measure of economic risk. By contrast, Conditional Value at Risk (CVaR) focuses on the lower tail of the distribution, quantifying average outcomes in the worst-case scenarios. So this model uses CVaR as the risk assessment tool (Rockafellar and Uryasev, 2000):

$$CVaR_\alpha(V) = \int_{-\infty}^{+\infty} z dF_V^\alpha(z) \qquad for\ \alpha \in [0,1] \tag{24}$$

$$F_V^\alpha(z) = \begin{cases} 0 & \text{when } z < VaR_\alpha(V) \\ \frac{F_V(z)-\alpha}{1-\alpha} & \text{when } z \geq VaR_\alpha(V) \end{cases} \tag{25}$$

where V refers to land values in this work, $z \in V$; α is confidence level; and $VaR_\alpha(V) = min\{z|F_V(z) \geq \alpha\}$ for $\alpha \in [0,1]$ (Linsmeier and Pearson, 2000). $CVaR_\alpha(V)$ represents the mean of the worst α fraction of outcomes, and it is continuous with respect to α and convex in V (Rockafellar and Uryasev, 2000). A detailed comparison between CVaR and VaR (another common tool for assessing downside risk) is provided in Appendix D.

2.6 Study Site

The model is designed for broad applicability across different aquifer systems, with flexibility to incorporate site-specific conditions. In this paper, it is demonstrated using a representative site informed by real-world data from the High Plains Aquifer (HPA) in Kansas. The following subsections describe the corresponding model setup.

2.6.1 High Plains Aquifer

The HPA is the largest freshwater aquifer system in the US, covering approximately 450,700 square kilometres, and underlying parts of eight states in the Great Plains from South Dakota to Texas (Gutentag, 1984). Approximately 30% of the groundwater used for irrigation in the U.S. comes from the HPA and approximately 20% of the irrigated land in the U.S. is located in the High Plains region (Sophocleous, 2005). Since the start of extensive irrigation development in the 1940s, groundwater levels have experienced a significant decline, with certain regions retaining less than 40% of their original saturated thickness (Steward and Allen, 2016; Whittemore et al., 2018). As a result, crop yields in the HPA may continue to level off or decline (Cotterman et al., 2018). Since groundwater is generally considered to be a a non-renewable resource without an available substitute, once it is depleted, there will be huge impacts on the quality of human life.

This paper focuses only on groundwater irrigation, as the area overlying the HPA in Kansas is a semi-arid region with limited surface-water supplies, where groundwater is used for 96% of the state's irrigated land (Butler Jr et al., 2018; Evett et al., 2020). Representative data from the HPA is used to demonstrate the model (Appendix B), making it adaptable and applicable to specific farms in this region and beyond, offering valuable guidance to irrigators in various locations.

2.6.2 Model Setup

To demonstrate the model, we initialized predefined state variables and applied Monte Carlo simulations to account for the stochastic components: precipitation and crop price. For each scenario, we calculated the expected present value of land at time zero under different variables. This study does not identify a universally optimal strategy, as only a limited set of irrigation strategies were tested due to computational constraints of the Monte Carlo approach. In principle, a theoretically optimal policy could be obtained by solving the Hamilton-Jacobi-Bellman (HJB) equation with finite difference methods (Insley and Wirjanto, 2010; Aghakazemjourabbaf and Insley, 2021; Yang, 2022), but such approaches are impractical in high-dimensional problems and limit the accessibility of the model. Instead, performance is assessed using CVaR, derived as the average of the worst 5% of outcomes, to capture lower-tail risks rather than universal optimality. In addition, we evaluate relative CVaR, expressed as the ratio of CVaR to the corresponding average land value, to highlight relative changes in downside risk.

Two planning horizons (T) were considered. The first is relatively short ($T = 20$ years), representing decisions by a farmer or regulator planning over the next two decades. The second extends until aquifer depletion ($T = TD$), effectively indicating the maximum duration farming can be sustained. This TD horizon approximates an infinite horizon, as further increases in T have negligible effects on outcomes.

Price simulations were run on a monthly time step. Because the model assumes the growing season in the HPA ends in September, corn prices from October are used to calculate annual cash flows. A 150-year time series of corn prices is simulated; if the operational period exceeds this duration, the price from the 150^{th} year is applied, as the present value of distant future cash flows becomes negligible due to discounting.

3 Results

This model demonstration examines how land values respond to variations in irrigation strategies, aquifer properties, and sustainable extraction rules. To capture these aspects, we selected and tested five variables representing decisions, regulatory, management, and physical conditions (Table 1).

Table 1: List and description of variables tested across scenarios.

Symbol	Description	Value Range	Explanation
β	Irrigation Fraction [-]	[0.5, 1]	Decision variable: farmer's direct irrigation decision
$\bar{I}$	Regulatory Pumping Limit [m^3/day]	[2000, 5000]	Conservation strategy: policy-imposed pumping cap
μ	Sustainable Extraction Rule [-]	[0.2, 1]	Conservation strategy: limit withdrawals of stored water
K	Hydraulic Conductivity [m/day]	[15, 40]	Hydrologic property affecting drawdown and pumping feasibility
s_y	Specific Yield [-]	[0.05, 0.35]	Hydrologic property affecting drawdown

Together, these variables illustrate how the model can assess trade-offs among farmers' decisions, policy limits, conservation strategies, and aquifer characteristics. For each scenario, 10,000 Monte Carlo simulations were performed to ensure statistical robustness and capture the range of possible outcomes under uncertainty. Each analysis isolates and tests a single objective to evaluate sensitivity. Unless stated otherwise, results assume a 2% discount rate.

3.1 Irrigation Strategies

In this section, we evaluate six groups of irrigation strategies (Table 2), designed to reflect local conditions and common irrigation practices, and representing a range of decision-making, regulatory, and management approaches: (A) no regulatory pumping limit ($\bar{I}$) with varying irrigation fractions (β); (B) constant regulatory pumping limits with varying irriga-

tion fractions; (C) time-varying pumping limits (two-stage) with a fixed irrigation fraction, following a large-to-small pattern; (D) time-varying pumping limits with a fixed irrigation fraction, following a small-to-large pattern; (E) time-varying irrigation fractions (two-stage) with a fixed pumping limit, following a large-to-small pattern; and (F) time-varying irrigation fractions with a fixed pumping limit, following a small-to-large pattern. The tested strategies draw from real-world irrigation practices, focusing on options that are both practically relevant and economically meaningful.

Table 2: Irrigation strategies.

Group	**Irrigation Fraction (β)**		**Regulatory Limit ($\bar{\imath}$)**	
	$t \leq T/2$	$t > T/2$	$t \leq T/2$	$t > T/2$
A1	1		-	
A2	0.9		1	
B1	1		[2000, 5000] (step 200)	
B2	0.9		[2000, 5000] (step 200)	
B3	0.8		[2000, 5000] (step 200)	
B4	0.5		[2000, 5000] (step 200)	
C1	1		4000	3500
C2	1		3900	3700
C3	1		3800	3600
D1	1		3500	4000
D2	1		3600	3800
D3	1		3700	3900
E1	1	0.9	3600	
E2	1	0.8	3600	
E3	1	0.7	3600	
E4	0.9	0.7	3600	
F1	0.9	1	3600	
F2	0.8	1	3600	
F3	0.7	1	3600	
F4	0.7	0.9	3600	

Figure 3 presents the expected land value and 95% CVaR results for Group B under $T = 20$ years and time to depletion (TD). In Figure 3d, the expected land value peaks at ~\$2.5 million when $\beta = 1$ (full irrigation) and the pumping limit is 3800 m^3/day. This represents the fair market value of the land if sold. Beyond this point, expected land value is largely insensitive to further increases in the pumping limit. At the same pumping limit, the 95% CVaR is ~\$1.9 million (In Figure 3e), indicating that in the worst 5% of cases, land value

could fall to roughly $1.9 million. When the irrigation fraction is in the range $\beta = 0.8 - 1$, land value initially increases with the regulatory pumping limit and then stabilizes, as the regulatory pumping rate exceeds the farmer's decision and no longer constrains pumping. However, when $\beta = 0.5$, the regulatory pumping limit does not constrain water use because actual irrigation remains fixed at 50% of crop water demand, resulting in relatively little variation in land value. The variations observed in Figures 3c and f arise because, when the pumping limit is ~2400 m^3/day, annual profits shift from negative to positive values, resulting in a small total land value and a large difference from the average, leading to a sudden change in the CVaR percentage. In addition to the main cases, we also evaluate a scenario with a 5% discount rate. Relative to the baseline 2% case, this generates a narrower range of land value and CVaR, but a greater relative CVaR. The higher discount rate places greater weight on near-term cash flows, reducing the present value of expected future income.

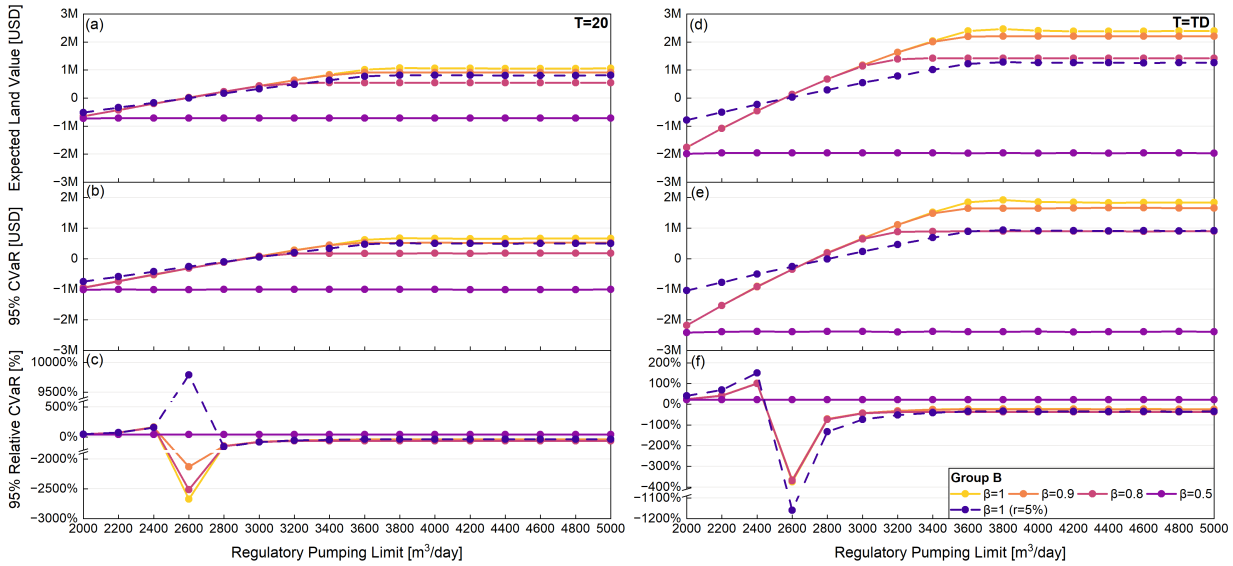

Figure 3: Expected land value, 95% CVaR and 95% relative CVaR under constant regulatory pumping limits with varying irrigation fractions (Group B). (a)-(c) T=20; (d)-(f) T=TD.

Figures 4a and c illustrate the relationship between expected land value and CVaR, with strategies (Table 2) labelled for comparison. Overall, higher expected land values are associated with higher CVaR results, indicating that increases in average land value also

correspond to better outcomes in the worst case scenario (bottom 5% of the distribution). Group C (front-loaded pumping with a higher limit in the early period) produces the largest values, particularly under $T = TD$, as discounting places greater weight on near-term income. For the scenarios with no regulatory limits, strategy A2, which applies 90% of crop water demand, yields substantially lower values than full-demand irrigation (A1). For the remaining strategies, differences in land value are relatively modest, generally less than 10%.

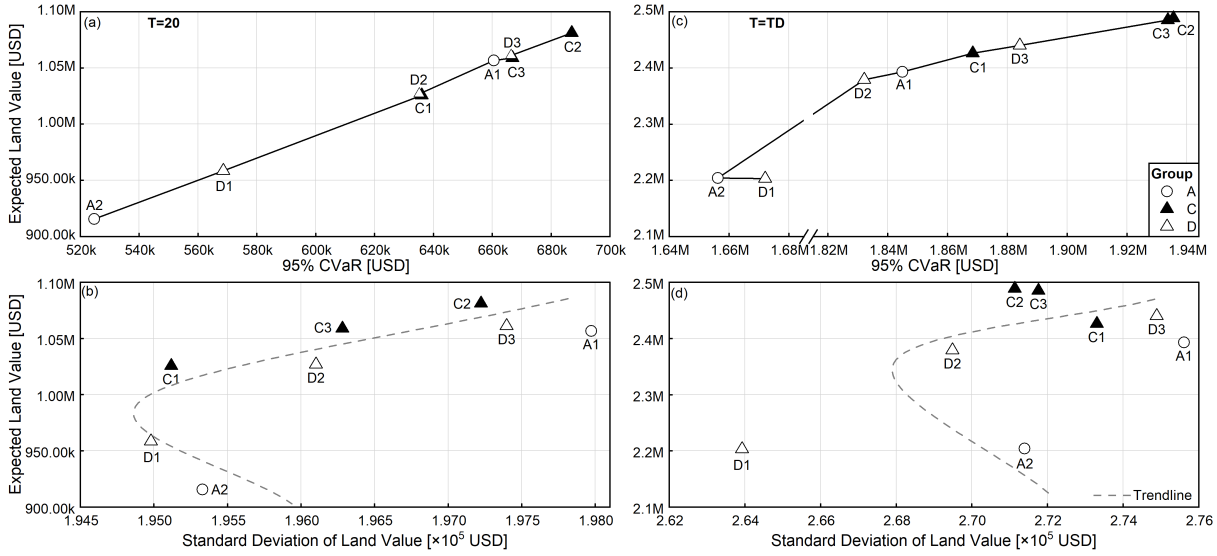

Figure 4: Relationships between expected land value and risk metrics: (a, c) 95% CVaR; (b, d) standard deviation, across irrigation strategies Groups A, C and D.

Figures 4b and d further illustrate these dynamics. Expected land values and standard deviations follow a characteristic concave ("C-shaped") pattern, with higher land values generally associated with greater risk.

For farmer's irrigation decision, the decision variable, we examined the effects of varying irrigation fractions (β) under $\mu = 1$ (Figure 5(a-c)). Expected land value and CVaR both increase with higher irrigation fractions, as greater water application enables more crop demand to be met. However, this gain comes at a cost: operational years decline sharply from 375 to 171 as β increases, illustrating the trade-off between short-term profitability and long-term resource availability. While $\beta = 0.9$ achieves ~90% of the full-irrigation land value

and ~80% of its CVaR, reducing β to 0.8 cuts land value nearly in half and reduces CVaR to ~30%. Below $\beta = 0.7$, land values fall to ~15% and CVaR becomes negative, highlighting increased downside risk and potential financial losses.

To explore dynamic decision-making, we tested eight irrigation strategies about β (Groups E and F in Table 2, Figure 5(d-g)). Strategies that start with higher β and gradually taper (Group E) consistently outperform others. In the $T = TD$ case, most strategies fall within a high-return/high-variability regime (top-right of Figure 5g), indicating that producers often face a trade-off between maximizing profitability and reducing interannual volatility. However, CVaR analysis shows an almost linear relationship with expected land value, indicating that lower mean returns are associated with worse downside outcomes. High pumping strategies result in increased variability: they generate high returns in favorable years but become more sensitive to unfavorable conditions (e.g., droughts, low prices). Notably, strategies with median land values also exhibit median CVaR, reflecting moderate downside risk, yet their standard deviations remain high. This highlights that variability captured by standard deviation does not necessarily reflect greater downside risk, results may fluctuate widely in the middle of the distribution without significantly worsening the worst-case outcomes.

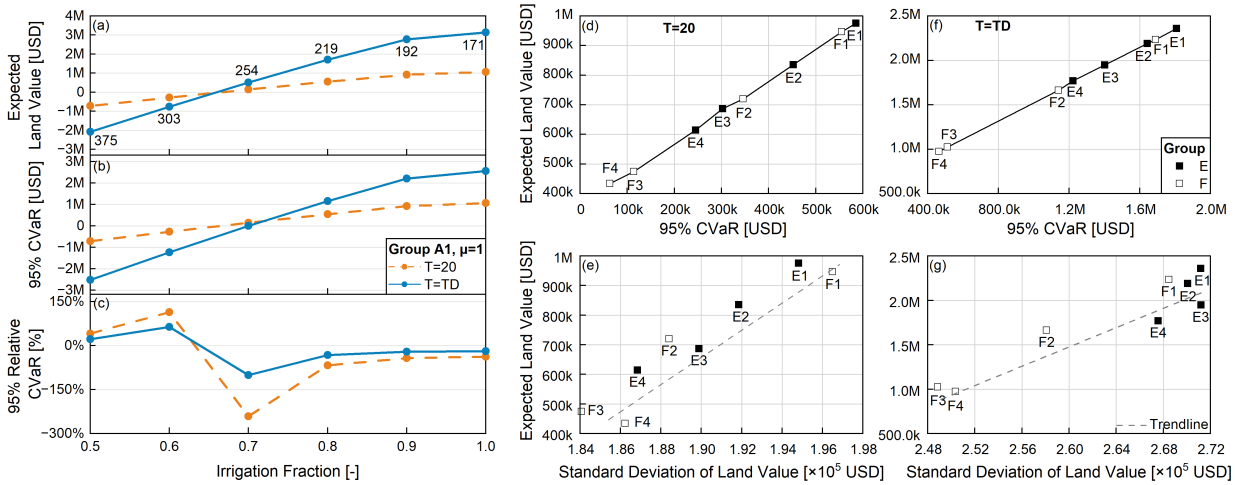

Figure 5: (a-c) Land values and CVaR results for different irrigation fractions, with labels showing operational years; (d-g) results for irrigation strategy Groups E and F.

In addition, we examined water depth dynamics under a constant regulatory pumping limit and full-demand irrigation (Group B1) over a 20-year horizon, with results summarized in Table 3. Differences across Monte Carlo simulations and under alternative pumping limits are not significant. This outcome is because in these simulations the 180-day non-pumping period in each year allows for substantial groundwater recovery. Moreover, given that the crop water demand (I_r) is around 3600 m^3/day, the tested pumping limits ($\bar{I}$) are relatively close to I_r. When repeated across 10,000 Monte Carlo simulations, the average actual pumping converges to similar values, leading to negligible differences in simulated water depth. It is anticipated that shorter recovery periods, or lower conductive materials that would require additional time to recover, leading to greater differences between these simulations.

Table 3: Simulated water depth under constant pumping limits and full-demand irrigation (Group B1, T=20)

$\bar{I}$ [m^3/day]	Max [m]	Min [m]	Mean [m]	Variance	Standard Deviation
3500	111.13	111.11	111.13	8.33E-07	9.13E-04
3600	111.23	111.20	111.23	6.88E-06	2.62E-03
3700	111.33	111.28	111.32	4.02E-05	6.34E-03
3800	111.43	111.34	111.40	1.60E-04	1.26E-02
3900	111.52	111.38	111.46	4.12E-04	2.03E-02
4000	111.58	111.39	111.49	7.17E-04	2.68E-02

3.2 Hydraulic Conductivity

In this section, we examined the effects of two key aquifer properties: hydraulic conductivity and specific yield. Hydraulic conductivity influences both groundwater drawdown and recovery, while specific yield primarily affects drawdown. For this analysis, no regulatory pumping limits are imposed, and irrigation decisions are assumed to fully meet crop water

demand for maximum yield (Group A1).

Figure 6(a1-c1) presents land value and CVaR results across different hydraulic conductivities. Over a 20-year horizon, both metrics increase slightly with higher conductivity. Greater hydraulic conductivity enhances aquifer recovery (Equation 6), improves water replenishment, and reduces drawdown (Equation 5), thereby lowering pumping costs and raising land values. When evaluated over the depletion horizon ($T = TD$), these effects become more noticeable: a conductivity of K = 10 m/day supports 52 years of operation, while K = 40 m/day extends this to 164 years. As shown in Figure 6(c1), the relative percentage differences decrease. These results confirm the role of aquifer properties in shaping economic outcomes, linking higher conductivity to greater returns and reduced risk.

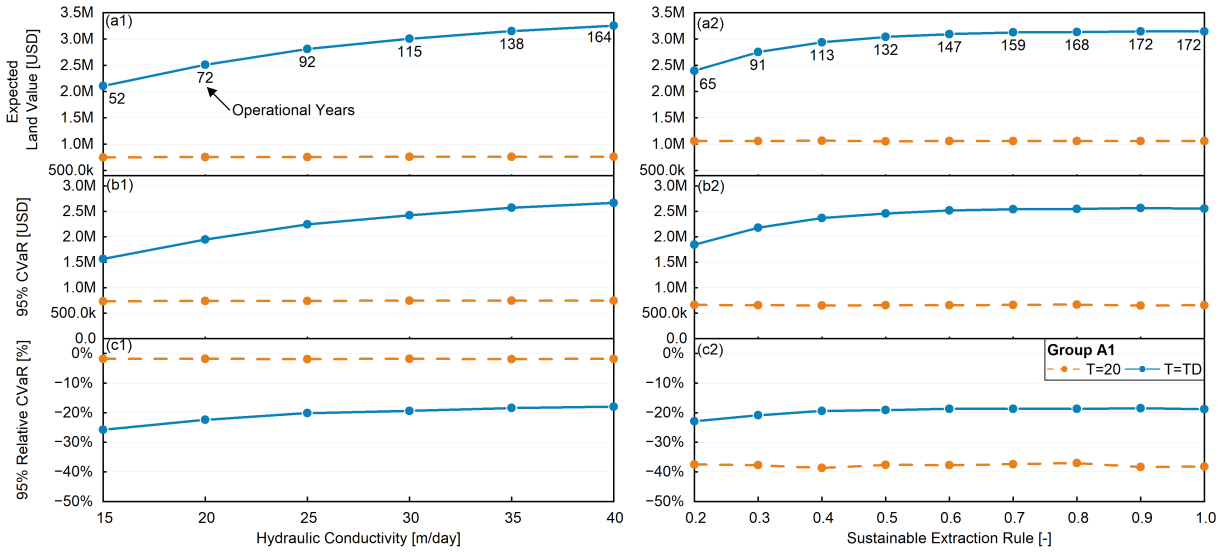

Figure 6: (a1-c1): Expected land values and CVaR results for different hydraulic conductivities; (a2-c2): Expected land values and CVaR results for different sustainable extraction rules.

However, the influence of specific yield on land value is less noticeable in our preliminary analysis. Variations in specific yield do not affect land value or CVaR across either planning horizon, as other physical constraints dominate the simulations. Supporting simulation results are provided in Appendix E.

3.3 Sustainable Extraction Rule

The sustainable extraction rule discussed in this section refers to the allowable proportion of groundwater use (μ). For example, if annual withdrawals are limited to 30% of the initial aquifer thickness (or hydraulic head) at the start of year 1, pumping continues through the growing season until the annual threshold is reached (i.e., conditional function in Figure 1), ensuring seasonal rather than mid-season cessation.

With a 20-year time frame, stored groundwater is sufficient to support irrigation, resulting in land value and CVaR being nearly identical as μ increases in Figure 6(a2-c2). However, when $T = TD$, land values and CVaR increase with relaxed extraction rules before stabilizing, and the relative CVaR decreases. At stricter sustainable extraction rules, relaxing the constraint ($\mu = 0.2 - 0.5$) leads to higher land values, as increased water availability significantly impacts both economic returns and associated risks. Despite this, even with an extension of operational years from 65 to 172 due to greater water availability, rising pumping costs and the effect of discounting future revenues contribute to a relatively stable expected land value over the long term.

4 Discussion

This study applies a newly developed hydro-economic model that uses Conditional Value-at-Risk (CVaR) and land values to examine how groundwater management strategies influence economic outcomes. By simulating a range of scenarios, the analysis identifies key relationships among groundwater use, land value, and financial risk.

For the demonstration case, a pumping limit of 3800 m^3/day generates the highest expected land values for most scenarios, since annual crop water demand ranges from 3600 to 3900 m^3/day depending on precipitation. Thus, setting the pumping limit at 3800 m^3/day

effectively balances water demand with sustainable extraction, providing both regulatory control and economic benefit. Across all irrigation strategies, allowing a larger pumping limit initially and then reducing it over time generates the highest expected land values in both $T = 20$ and $T = TD$ cases. This outcome arises because discounting places greater weight on near-term revenues.

For farmers' direct decisions (β), higher irrigation fractions generally raise land values by better meeting crop water demand. Irrigation of less than 80% of water demand is not optimal for the farmer, but the marginal benefits diminish sharply between 0.9 and 1.0. Although shorter operational periods can generate higher near-term value, this approach compromises long-term sustainability by leaving less water for future generations as indicated by the time to aquifer depletion and reducing flexibility to address emerging challenges.

CVaR analysis shows that strategies with higher expected land values are also associated with lower risk (higher CVaR), indicating that improvements in average returns are accompanied by stronger performance under unfavorable conditions. Unlike standard deviation, which captures both upward and downward variability, CVaR focuses on the lower tail of the distribution and therefore provides a clearer measure of downside risk. This makes CVaR a more informative tool for identifying management options that safeguard against unfavorable scenarios, rather than penalizing strategies simply because they exhibit greater overall variability.

Due to faster aquifer recovery and smaller drawdown, higher hydraulic conductivity enhances both land values and CVaR for $T = 20$ and TD cases, reflecting reduced financial risk as groundwater availability improves. This positive correlation highlights the importance of aligning pumping rules with aquifer properties to sustain farm-level economic stability under variable conditions. This model assumes a homogeneous aquifer and does not include boundary conditions such as connections with streams or lakes. The water from infiltration that remains in the vadose zone is not considered in this study, though it is important in

supporting crop growth. A more detailed 2D or 3D hydrologic numerical model could better capture groundwater dynamics; however, this study prioritizes an easily accessible approach that minimizes data, technical, and financial requirements.

The results of sustainable extraction rules suggest that greater water availability does not always lead to higher land values. When $\mu > 0.5$, diminishing returns occur, additional water use only provides limited economic benefit. This implies that regulators may have flexibility to reduce allowable extraction without significantly compromising farm profitability. Such adjustments could support long-term aquifer sustainability while mitigating risks of over-extraction.

5 Conclusion

This study introduces and demonstrates a farm-level hydro-economic model that couples groundwater dynamics with economic outcomes to evaluate irrigation strategies under physical and regulatory constraints. By incorporating Conditional Value-at-Risk (CVaR), the model captures not only average outcomes but also downside risks, offering a more robust basis for decision-making. Results show that higher pumping does not necessarily increase revenues or reduce risks, as diminishing returns and aquifer depletion can offset short-term gains, while aquifer properties critically shape both profitability and risk exposure. The analysis highlights that today's extraction choices directly shape the economic viability of farms for future generations as indicated by the time to depletion of the aquifer. Designed to be adaptable to site-specific conditions, this model provides a practical tool for farmers, policymakers, and regulators seeking to align irrigation decisions with long-term groundwater sustainability.

6 Author Contributions

B.T.: Conceptualization, Methodology, Data curation, Software, Validation, Visualization, Writing – original draft, Writing – review and editing. A.B.: Conceptualization, Methodology, Validation, Supervision, Writing – review and editing, Project administration, Funding acquisition. M.I.: Methodology, Validation, Supervision, Writing – review and editing.

7 Funding Sources

This work was supported by a University of Waterloo Water Institute Seed Grant; University of Waterloo Trailblazer Award; and the Natural Sciences and Engineering Research Council of Canada [Discovery Grant].

References

Abramowitz, M. and Stegun, I. A. (1968), *Handbook of mathematical functions with formulas, graphs, and mathematical tables*, Vol. 55, US Government printing office.

Aeschbach-Hertig, W. and Gleeson, T. (2012), 'Regional strategies for the accelerating global problem of groundwater depletion', *Nat. Geosci.* **5**(12), 853–861.

Aghakazemjourabbaf, S. and Insley, M. (2021), 'Leaving your tailings behind: Environmental bonds, bankruptcy and waste cleanup', *Resource and Energy Economics* **65**, 101246.

Agriculture and Agri-Food Canada (n.d.), http://www4.agr.gc.ca/AAFCAAC/display-afficher.do?id=1295963199087&lang=eng. Accessed: 2022-5-10.

Akhtar, N., Syakir Ishak, M. I., Bhawani, S. A. and Umar, K. (2021), 'Various natural and anthropogenic factors responsible for water quality degradation: A review', *Water* **13**(19), 2660.

Alam, M. F., Pavelic, P., Sikka, A., Krishnan, S., Dodiya, M., Bhadaliya, P. and Joshi, V. (2023), 'Energy consumption as a proxy to estimate groundwater abstraction in irrigation', *Groundwater for Sustainable Development* **23**, 101035.

Allen, R. G., Pereira, L. S., Raes, D. and Smith, M. (1998), 'Crop evapotranspiration-guidelines for computing crop water requirements-FAO irrigation and drainage paper 56', *FAO - Food and Agriculture Organization of the United Nations, Rome* **300**(9).

Amaya, M., Baran, A., Lopez-Morales, C. and Little, J. C. (2021), 'A coupled hydrologic-economic modeling framework for scenario analysis', *Frontiers in Water* **3**, 681553.

Ansaripoor, A. H., Oliveira, F. S. and Liret, A. (2014), 'A risk management system for sustainable fleet replacement', *European Journal of Operational Research* **237**(2), 701–712.

Brookfield, A. (2016), 'Minimum saturated thickness calculator', *Kansas Geological Survey Open-File Report* **3**.

Butler Jr, J., Bohling, G., Whittemore, D. and Wilson, B. (2020), 'Charting pathways toward sustainability for aquifers supporting irrigated agriculture', *Water Resources Research* **56**(10), e2020WR027961.

Butler Jr, J. J., Whittemore, D. O., Wilson, B. B. and Bohling, G. C. (2018), 'Sustainability of aquifers supporting irrigated agriculture: A case study of the high plains aquifer in kansas', *Water International* **43**(6), 815–828.

Cao, G., Zheng, C., Scanlon, B. R., Liu, J. and Li, W. (2013), 'Use of flow modeling to assess sustainability of groundwater resources in the north china plain', *Water Resources Research* **49**(1), 159–175.

Case, C., Pidcoe, W. and Fenske, P. (1974), 'Theis equation analysis of residual drawdown data', *Water Resources Research* **10**(6), 1253–1256.

Chapuis, R. P. (1992), 'Using cooper-jacob approximation to take account of pumping well pipe storage effects in early drawdown data of a confined aquifer', *Groundwater* **30**(3), 331–337.

Cooper, H. and Jacob, C. E. (1946), 'A generalized graphical method for evaluating formation constants and summarizing well-field history', *Eos, Transactions American Geophysical Union* **27**(4), 526–534.

Cotterman, K. A., Kendall, A. D., Basso, B. and Hyndman, D. W. (2018), 'Groundwater depletion and climate change: future prospects of crop production in the central high plains aquifer', *Clim. Change* **146**(1-2), 187–200.

Crosbie, R. S., Scanlon, B. R., Mpelasoka, F. S., Reedy, R. C., Gates, J. B. and Zhang, L. (2013), 'Potential climate change effects on groundwater recharge in the high plains aquifer, usa', *Water Resources Research* **49**(7), 3936–3951.

Ding, Y. and Peterson, J. M. (2012), 'Comparing the cost-effectiveness of water conservation policies in a depleting aquifer: A dynamic analysis of the kansas high plains', *Journal of Agricultural and Applied Economics* **44**(2), 223–234.

Driscoll, F. G. (1986), 'Groundwater and wells', *St. Paul* .

Edwards, E. C. (2016), 'What lies beneath? aquifer heterogeneity and the economics of groundwater management', *J. Assoc. Environ. Resour. Econ.* **3**(2), 453–491.

Escriva-Bou, A., Hui, R., Maples, S., Medellín-Azuara, J., Harter, T. and Lund, J. (2020), 'Planning for groundwater sustainability accounting for uncertainty and costs: An application to california's central valley', *Journal of environmental management* **264**, 110426.

Evett, S. R., Colaizzi, P. D., Lamm, F. R., O'Shaughnessy, S. A., Heeren, D. M., Trout, T. J., Kranz, W. L. and Lin, X. (2020), 'Past, present, and future of irrigation on the us great plains', *Transactions of the ASABE* **63**(3), 703–729.

Ferris, J. (1963), 'Methods of determining permeability, transmissivity and drawdown', *US Geol. Surv. Water Supply Paper* pp. 1536–1.

Filippi, C., Guastaroba, G. and Speranza, M. G. (2020), 'Conditional value-at-risk beyond finance: a survey', *International Transactions in Operational Research* **27**(3), 1277–1319.

Fróna, D., Szenderák, J. and Harangi-Rákos, M. (2019), 'The challenge of feeding the world', *Sustainability* **11**(20), 5816.

Genova, P. and Wei, Y. (2023), 'A socio-hydrological model for assessing water resource allocation and water environmental regulations in the maipo river basin', *Journal of Hydrology* **617**, 129159.

Gotoh, J.-y. and Takano, Y. (2007), 'Newsvendor solutions via conditional value-at-risk minimization', *European Journal of Operational Research* **179**(1), 80–96.

Guilfoos, T., Khanna, N. and Peterson, J. M. (2016), 'Efficiency of viable groundwater management policies', *Land Econ.* **92**(4), 618–640.

Gurdak, J. J. and Roe, C. D. (2010), 'Recharge rates and chemistry beneath playas of the high plains aquifer, usa', *Hydrogeology Journal* **18**(8), 1747.

Gutentag, E. D. (1984), *Geohydrology of the High Plains aquifer in parts of Colorado, Kansas, Nebraska, New Mexico, Oklahoma, South Dakota, Texas, and Wyoming*, number 1400, US Government Printing Office.

Hemathilake, D. and Gunathilake, D. (2022), Agricultural productivity and food supply to meet increased demands, *in* 'Future foods', Elsevier, pp. 539–553.

Hosseini-Firouz, M. (2013), 'Optimal offering strategy considering the risk management for wind power producers in electricity market', *International Journal of Electrical Power & Energy Systems* **49**, 359–368.

Ibendahl, G., O'Brien, D., Lancaster, S., Holman, J. and Haag, L. (2023), 'Corn cost-return budget (w-c-f rotation) in southwest kansas', https://agmanager.info/farm-budgets/2024-farm-management-guides-irrigated-crops. Accessed: 2024-08-22.

Insley, M. (2002), 'A real options approach to the valuation of a forestry investment', *Journal of environmental economics and management* **44**(3), 471–492.

Insley, M. C. and Wirjanto, T. S. (2010), 'Contrasting two approaches in real options valuation: contingent claims versus dynamic programming', *Journal of Forest Economics* **16**(2), 157–176.

Jain, M., Fishman, R., Mondal, P., Galford, G. L., Bhattarai, N., Naeem, S., Lall, U., Balwinder-Singh and DeFries, R. S. (2021), 'Groundwater depletion will reduce cropping intensity in india', *Science advances* **7**(9), eabd2849.

Jia, H., Qian, H., Zheng, L., Feng, W., Wang, H. and Gao, Y. (2020), 'Alterations to groundwater chemistry due to modern water transfer for irrigation over decades', *Science of the Total Environment* **717**, 137170.

Juenemann, S. and Zimmerman, R. (2021), 'Colby weather reports.', https://www.wkrec.org/weather/colby_weather.html. Accessed: 2022-5-10.

Kansas Geological Survey (n.d.), https://www.kgs.ku.edu/. Accessed: 2023-7-10.

Kansas Mesonet (n.d.), 'Max/min weather data', https://mesonet.k-state.edu/weather/maxmin/. Accessed: 2022-5-10.

Katic, P. and Grafton, R. Q. (2011), 'Optimal groundwater extraction under uncertainty: resilience versus economic payoffs', *Journal of Hydrology* **406**(3-4), 215–224.

Klocke, N. L. (2011), 'Development of crop production functions for irrigation in north central kansas'.

Konikow, L. F. (2015), 'Long-term groundwater depletion in the united states', *Groundwater* **53**(1), 2–9.

Lamm, F. (2021), 'Monthly, seasonal, and yearly precipitation amounts (inches) recorded at colby, kansas weather stations.', https://www.ksre.k-state.edu/irrigate/et/PRECIPSum.pdf. Accessed: 2022-5-10.

Linsmeier, T. J. and Pearson, N. D. (2000), 'Value at risk', *Financial analysts journal* **56**(2), 47–67.

Mancosu, N., Snyder, R. L., Kyriakakis, G. and Spano, D. (2015), 'Water scarcity and future challenges for food production', *Water* **7**(3), 975–992.

Martin, D. L., Supalla, R. J., Thompson, C. L., McMullen, B. P., Hergert, G. W. and Burgener, P. A. (2010), Advances in deficit irrigation management, *in* '5th National Decennial Irrigation Conference Proceedings, 5-8 December 2010, Phoenix Convention Center, Phoenix, Arizona USA', American Society of Agricultural and Biological Engineers, p. 1.

Meixner, T., Manning, A. H., Stonestrom, D. A., Allen, D. M., Ajami, H., Blasch, K. W., Brookfield, A. E., Castro, C. L., Clark, J. F., Gochis, D. J., Flint, A. L., Neff, K. L., Niraula, R., Rodell, M., Scanlon, B. R., Singha, K. and Walvoord, M. A. (2016), 'Implications of projected climate change for groundwater recharge in the western united states', *J. Hydrol. (Amst.)* **534**, 124–138.

Merrill, N. H. and Guilfoos, T. (2018), 'Optimal groundwater extraction under uncertainty and a spatial stock externality', *American journal of agricultural economics* **100**(1), 220–238.

Miller, J. A. and Appel, C. L. (1997), Ground water atlas of the united states: Segment 3, kansas, missouri, nebraska, Technical report, US Geological Survey.

Mukherjee, A., Scanlon, B. R., Aureli, A., Langan, S., Guo, H. and McKenzie, A. (2021), Global groundwater: from scarcity to security through sustainability and solutions, *in* 'Global groundwater', Elsevier, pp. 3–20.

Neuman, S. P. (1975), 'Analysis of pumping test data from anisotropic unconfined aquifers considering delayed gravity response', *Water Resour. Res.* **11**(2), 329–342.

Oehninger, E. B. and Lawell, C.-Y. C. L. (2019), 'Property rights and groundwater management in the high plains aquifer', *Resource and Energy Economics* **63**.

Pousinho, H. M. I., Mendes, V. M. F. and Catalão, J. P. d. S. (2011), 'A risk-averse optimization model for trading wind energy in a market environment under uncertainty', *Energy* **36**(8), 4935–4942.

Rajan, N., Maas, S., Kellison, R., Dollar, M., Cui, S., Sharma, S. and Attia, A. (2015), 'Emitter uniformity and application efficiency for centre-pivot irrigation systems', *Irrigation and Drainage* **64**(3), 353–361.

Richardson, C. W. (1981), 'Stochastic simulation of daily precipitation, temperature, and solar radiation', *Water Resour. Res.* **17**(1), 182–190.

Rockafellar, R. T. and Uryasev, S. (2000), 'Optimization of conditional value-at-risk', *Journal of risk* **2**, 21–42.

Rockafellar, R. T. and Uryasev, S. (2002), 'Conditional value-at-risk for general loss distributions', *Journal of banking & finance* **26**(7), 1443–1471.

Romeijn, H. E., Ahuja, R. K., Dempsey, J. F. and Kumar, A. (2006), 'A new linear programming approach to radiation therapy treatment planning problems', *Operations Research* **54**(2), 201–216.

Sacks, W. J., Cook, B. I., Buenning, N., Levis, S. and Helkowski, J. H. (2009), 'Effects of global irrigation on the near-surface climate', *Clim. Dyn.* **33**(2-3), 159–175.

Sarykalin, S., Serraino, G. and Uryasev, S. (2008), Value-at-risk vs. conditional value-at-risk in risk management and optimization, *in* 'State-of-the-art decision-making tools in the information-intensive age', Informs, pp. 270–294.

Sawik, T. (2019), 'Disruption mitigation and recovery in supply chains using portfolio approach', *Omega* **84**, 232–248.

Schwartz, F. W. and Ibaraki, M. (2011), 'Groundwater: A resource in decline', *Elements* **7**(3), 175–179.

Siebert, S., Burke, J., Faures, J.-M., Frenken, K., Hoogeveen, J., Döll, P. and Portmann, F. T. (2010), 'Groundwater use for irrigation-a global inventory', *Hydrology and earth system sciences* **14**(10), 1863–1880.

Sophocleous, M. (2005), 'Groundwater recharge and sustainability in the high plains aquifer in kansas, usa', *Hydrogeology Journal* **13**, 351–365.

Sophocleous, M. (2010), 'groundwater management practices, challenges, and innovations in the high plains aquifer, usa–lessons and recommended actions', *Hydrogeology Journal* **18**(3), 559.

Stanton, J. (2013), 'Ds-777 average annual recharge, 2000 to 2009, in inches estimated from the soil water balance (swb) model for the high plains aquifer in parts of colorado, kansas, nebraska, new mexico, oklahoma, south dakota, texas, and wyoming: U.s. geological survey data release', https://doi.org/10.5066/P9K0H7I0. Accessed: 2024-11-02.

Steward, D. R. and Allen, A. J. (2016), 'Peak groundwater depletion in the high plains aquifer, projections from 1930 to 2110', *Agric. Water Manag.* **170**, 36–48.

Theis, C. V. (1935), 'The relation between the lowering of the piezometric surface and the rate and duration of discharge of a well using ground-water storage', *Eos, Transactions American Geophysical Union* **16**(2), 519–524.

Toumazis, I. and Kwon, C. (2013), 'Routing hazardous materials on time-dependent networks using conditional value-at-risk', *Transportation Research Part C: Emerging Technologies* **37**, 73–92.

Tzanakakis, V. A., Paranychianakis, N. V. and Angelakis, A. N. (2020), 'Water supply and water scarcity'.

U.S. Bureau of Labor Statistic (2024), 'Consumer Price Index', https://www.bls.gov/cpi/. Accessed: 2024-10-01.

U.S. Drought Monitor (n.d.), https://droughtmonitor.unl.edu/. Accessed: 2023-7-10.

U.S. Energy Information Administration (2024), 'Average price of electricity to ultimate customers by end-use sector', https://www.eia.gov/electricity/monthly. Accessed: 2024-11-02.

U.S. Geological Survey (n.d.), https://www.usgs.gov/. Accessed: 2023-7-10.

USDA (2024), 'Prices Received: Corn Prices Received by Month, US', https://www.nass.usda.gov/Charts_and_Maps/Agricultural_Prices/pricecn.php. Accessed: 2024-10-01.

Water Security Agency (2020), https://www.wsask.ca/. Accessed: 2023-7-10.

Whittemore, D. O., Butler Jr, J. J. and Wilson, B. B. (2018), 'Status of the high plains aquifer in kansas', *Kansas Geological Survey Technical Series* **22**, 1–28.

Wu, T. and Blackhurst, J. V. (2009), *Managing supply chain risk and vulnerability: tools and methods for supply chain decision makers*, Springer Science & Business Media.

Yamout, G. M., Hatfield, K. and Romeijn, H. E. (2007), 'Comparison of new conditional value-at-risk-based management models for optimal allocation of uncertain water supplies', *Water Resour. Res.* **43**(7).

Yang, X. (2022), An analysis of optimal agricultural fertilizer application decisions in the presence of market and weather uncertainties and nutrient pollution, PhD thesis, University of Waterloo.

Zhang, D., Xu, H. and Wu, Y. (2009), 'Single and multi-period optimal inventory control models with risk-averse constraints', *European Journal of Operational Research* **199**(2), 420–434.

Zhang, K., Nieto, A. and Kleit, A. N. (2015), 'The real option value of mining operations using mean-reverting commodity prices', *Mineral Economics* **28**, 11–22.

A Hydrologic Components

A.1 Precipitation

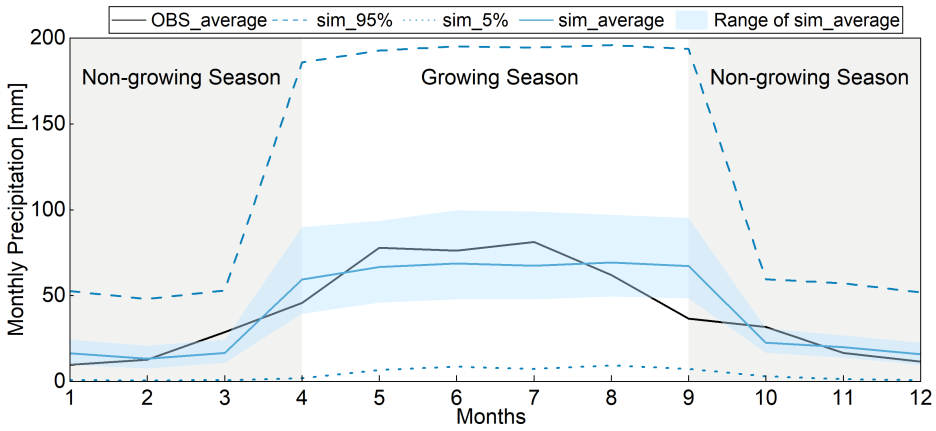

Figure A-1: Simulated and observed monthly precipitation: OBS-average (observed), sim-95% and sim-5% (simulated 95th and 5th percentiles), sim-average (simulated average), and range of simulated average.

A.2 Aquifer Drawdown

In unconfined aquifers, drawdown can be corrected due to the decreasing aquifer thickness using the following equation for corrected drawdown (S_c $[L]$) (Ferris, 1963):

$$S_c - \frac{(S_c)^2}{2b} = S_{aquifer} \tag{A-1}$$

S_{eff} $[L]$ represents the additional drawdown due to energy losses by inefficient wells. W_{eff} is the well efficiency as a percentage $[L^0]$.

$$S_{eff} = \left(\frac{100}{W_{eff}} - 1\right) \times S_c \tag{A-2}$$

Pumping from neighboring wells can also impact the target well's drawdown under multi-well scenarios. Abramowitz and Stegun (1968) proposed a method that can estimate the

additional drawdown due to neighboring pumping wells ($S_{neighbor}$ $[L]$).

$$S_{neighbor} = \frac{Q_n}{4\pi T_{aquifer}} \left[-0.5772 - \ln u + u + 0.25u^2 + 0.05556u^3 - 0.01042u^4 + 0.001667u^5 \right] \tag{A-3}$$

where $u = \frac{r_n^2 s_y}{4Tt_n}$, Q_n is the pumping rate of the neighboring wells $[L^3T^{-1}]$, which is assumed equal to Q; r_n is the distance from the target well to the neighboring wells $[L]$; t_n is the duration of pumping at the neighboring wells $[T]$.

Equation 5 assumes that the hydraulic head does not change with pumping in a confined aquifer; therefore, corrections for unconfined systems are (Ferris, 1963):

$$S_{c-all} - \frac{(S_{c-all})^2}{2b} = S_{aquifer} + S_{neighbor} \tag{A-4}$$

The total drawdown (S_{total} $[L]$) is the sum of corrected drawdown (S_{c-all}) and the additional drawdown due to well losses (S_{eff}):

$$S_{total} = S_{c-all} + S_{eff} \tag{A-5}$$

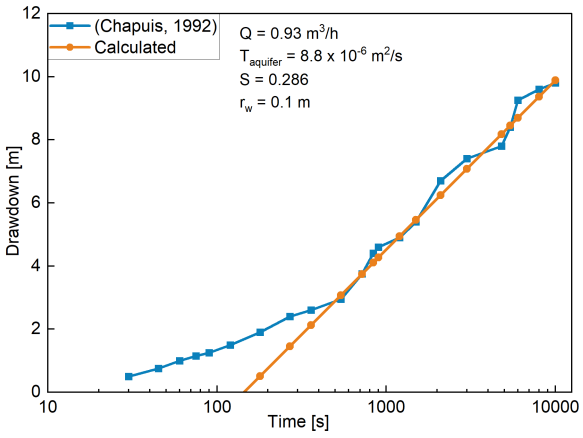

Figure A-2: Comparison of Chapuis (1992) drawdown data and calculated results, demonstrating a good fit with late-time data.

A.3 Groundwater Recovery

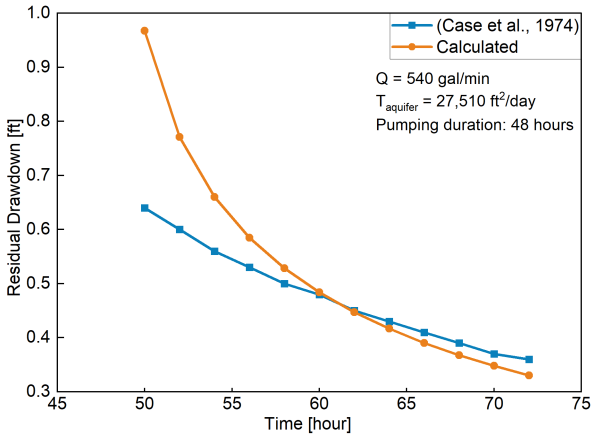

Figure A-3: Comparison of Case et al. (1974) recovery data and calculated results, demonstrating a good fit with late-time data.

A.4 Crop Yield

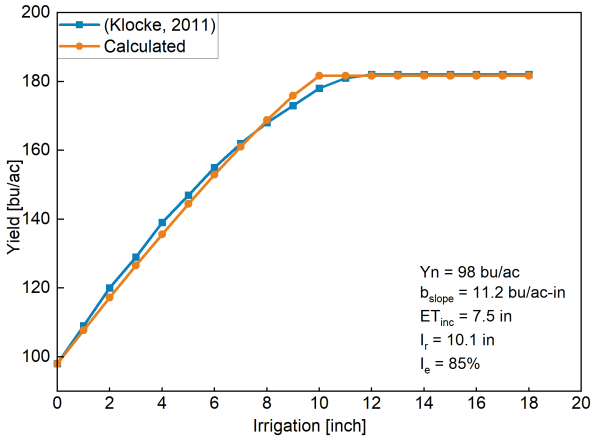

Figure A-4: Comparison of Klocke (2011) crop yield data and calculated results.

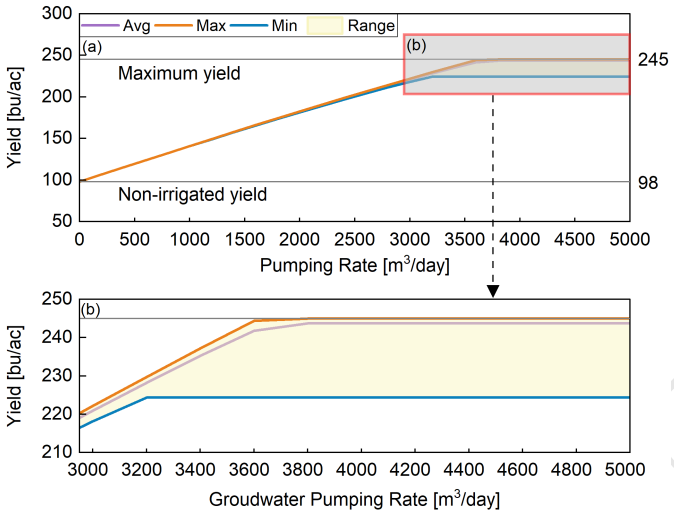

Figure A-5: (a) Annual yield at different pumping rates; (b) Zoomed-in view for pumping rates between 3000 and 5000 m^3/day.

B Parameters

Table B-1: Input parameter values.

Parameters	Description (Units)	Reference	Value	Source
λ_{grow}	Distribution parameter for growing season (-)	Eqn 3	0.0158	Lamm (2021)
$\lambda_{non-grow}$	Distribution parameter for non-growing season (-)	Eqn 3	0.0541	Lamm (2021)
I_e	Irrigation efficiency, center pivot irrigation system (-)	Eqn 4	0.9	Rajan et al. (2015)
P_e	Precipitation efficiency (-)	Eqn 4	0.8	AE
R_{ch}	Recharge rate ($m \cdot yr^{-1}$)	Eqn 4	0.0228	Stanton (2013)
r_w	Effective radius of the well (m)	Eqn 5	0.7	AE
s_y	Aquifer specific yield (-)	Eqn 5	0.15	U.S. Geological Survey (n.d.)
t_p	Duration of pumping (day)	Eqn 5	180	AE
b_t	Aquifer saturated thickness (m)	Eqn 5	60.96[a]	U.S. Geological Survey (n.d.)
t_s	Time since the start of pumping (day)	Eqn 6	360	AE
t_c	Time since the start of cessation (day)	Eqn 6	180	AE
ET_r	Reference ET ($mm \cdot yr^{-1}$)	Eqn 7	553.45[b]	AE
K_c	Daily crop coefficient, corn (-)	Eqn 8	1.2	Allen et al. (1998)
Y_n	Non-irrigated yield (bushel per acre)	Eqn 9	98	Klocke (2011)
b_{slope}	Slope of the yield-evapotranspiration function (bushel per acre per inch)	Eqn 9	11.2	Klocke (2011)
$c(1)$	OLS parameter (-)	Eqn 14	-0.04114	-
$c(2)$	OLS parameter (-)	Eqn 14	0.2049	-
θ	Speed of mean reversion (-)	Eqn 14	0.4937	-
se_m	OLS parameter (-)	Eqn 14	0.05168	-
σ_m	Volatility (-)	Eqn 14	0.179	-
$\bar{P}$	Long-run mean (USD)	Eqn 14	4.982	USDA (2024)

ρ	Water density ($kg \cdot m^{-3}$)	Eqn 15	1000	-
g	Gravity factor ($m \cdot s^{-2}$)	Eqn 15	9.81	-
η_p	Pumping efficiency (-)	Eqn 15	0.8	AE
C_y	Fertilizer cost (USD per bushel)	Eqn 21	0.71	Ibendahl et al. (2023)
C_f	Fixed cost (USD per acre)	Eqn 21	820.35	Ibendahl et al. (2023)
C_e	Electricity Price (USD per kWh)	Eqn 21	0.12	U.S. Energy Information Administration (2024)
W_{eff}	Well efficiency (-)	Eqn A-2	0.8	AE
r_n	Distance from the target well to the neighboring wells (m)	Eqn A-3	100	AE

[a] Initial aquifer saturated thickness before pumping.

[b] Estimated ET_r from Eqn 7. General data for the representative HPA site are taken from Juenemann and Zimmerman (2021).

[*] Authors' elaboration (AE). These data are referenced from U.S. Geological Survey (n.d.); Kansas Geological Survey (n.d.); Kansas Mesonet (n.d.); Water Security Agency (2020); U.S. Drought Monitor (n.d.); Agriculture and Agri-Food Canada (n.d.). Detailed data and code will be provided online. For additional information, please contact the authors.

C Price

For the HPA site, we use monthly corn price data (January 2015 to May 2024) from the USDA (2024), deflated using the U.S. Consumer Price Index (CPI) provided by the U.S. Bureau of Labor Statistic (2024). We conducted 10,000 Monte Carlo simulations based on the price model; results are shown in Figure C-1. To further validate the price model, we applied Maximum Likelihood Estimation (MLE) (Yang, 2022). The estimated standard errors of the model parameters for the corn price process are as follows: $se_\theta = 0.3283$, $se_{\bar{P}} = 0.5863$ and $se_\sigma = 0.0119$. The corresponding simulation results using MLE-estimated parameters are presented in Figure C-2.

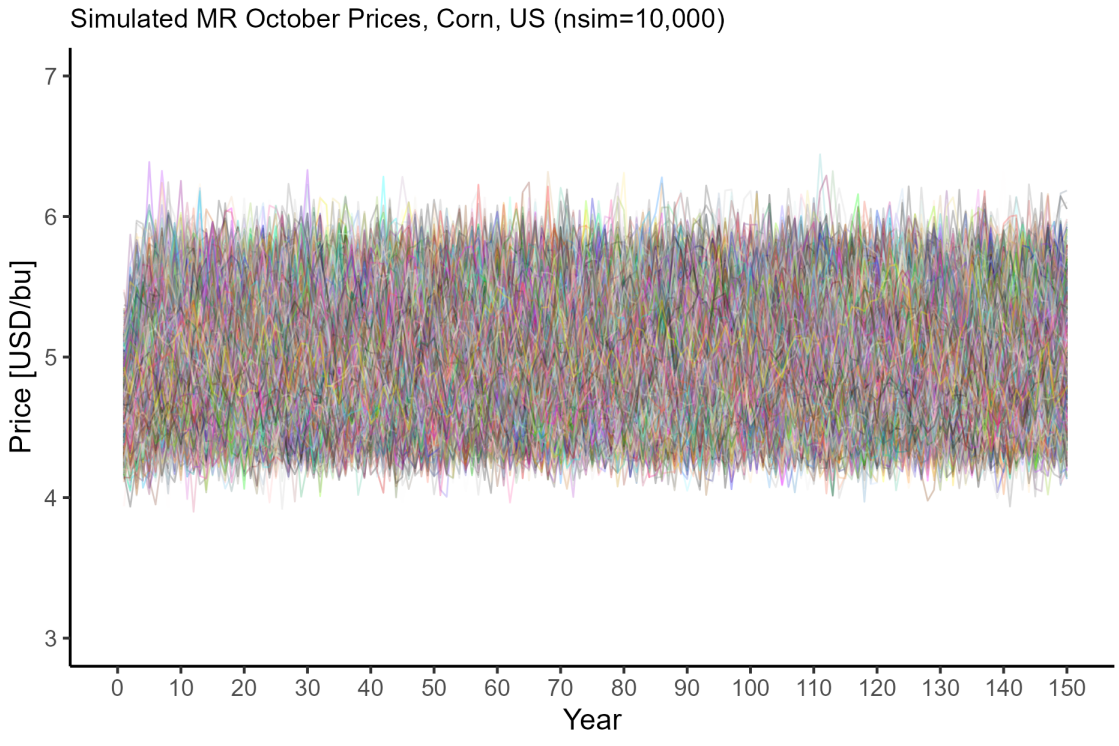

Figure C-1: Price estimations of 10,000 times Monte Carlo simulation for HPA.

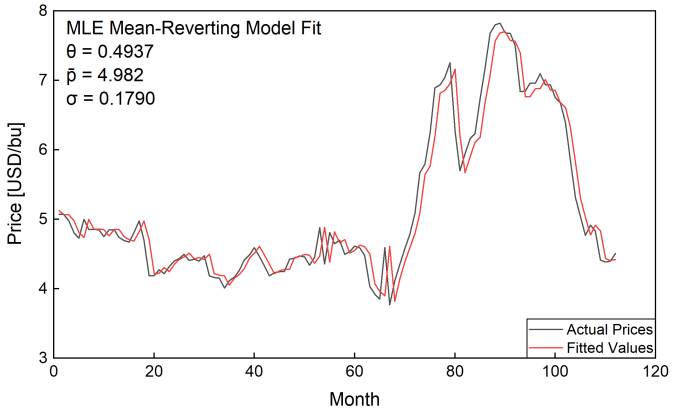

Figure C-2: MLE simulated data and historical prices, HPA. Note: The one-year shift occurs because the simulation requires an initial year to establish the starting price.

D CVaR and VaR

CVaR quantifies tail risks rather than risk at a single confidence level (Figure D-1a). Figure D-1b compares VaR and CVaR calculated for a scenario run for the HPA, presenting three confidence levels. CVaR consistently has greater negative values than VaR under the same conditions, highlighting its focus on the increased tail risks caused by fluctuations in precipitation, costs, and crop prices. This makes CVaR particularly useful for analyzing nonlinear systems, such as contaminant transport and groundwater problems, where risk is measured in non-monetary terms (Yamout et al., 2007).

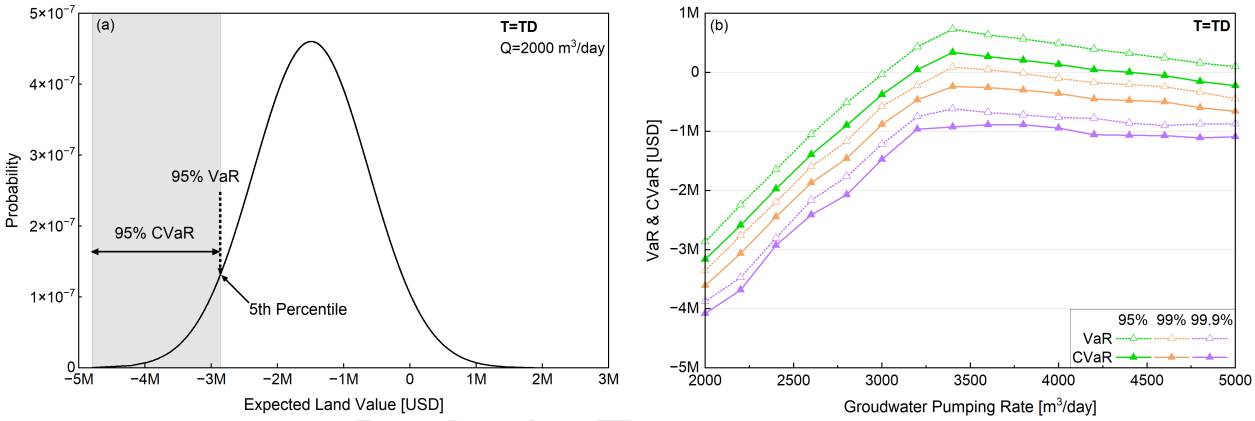

Figure D-1: (a) Normal distribution of expected land value for a hypothetical site; (b) illustration of VaR and CVaR.

E Specific Yield

The operational lifetime remains fixed at 65 years across different specific yield values. This occurs because the simulation terminates once the sustainable extraction rule is triggered, i.e., when aquifer thickness falls below the pumping threshold. Variations in relative CVaR are minor and primarily reflect stochastic precipitation and price fluctuations. Overall, specific yield proves to be an insensitive parameter in this model.

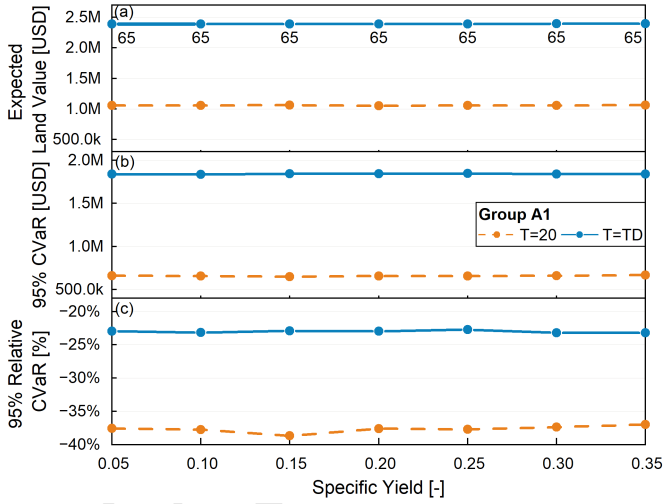

Figure E-1: (a) Land values, (b) 95% CVaR, and (c) relative CVaR for different specific yields.